DYNAMICS OF DUST IN A PLASMA SHEATH AND INJECTION OF DUST INTO THE PLASMA SHEATH ABOVE MOON AND ASTEROIDAL SURFACES

TORE NITTER and OVE HAVNES

The Auroral Observatory, University of Tromsø, Tromsø, Norway

(Received 18 June, 1991)

Abstract. We have examined single dust particle dynamics in a plasma sheath near the surface of solid bodies in space, considering conditions which resemble those of planetary system bodies, when photoelectric effect can be neglected. The forces on the dust particles are assumed to be from the electric field in the sheath and from gravitation only. As the dust particles will charge negatively in the sheath, these forces will act in opposite directions and may balance.

The charge delay of a moving dust particle is responsible for many of the interesting dynamical properties, and we show that for a stationary plasma, dust motion is unstable to about one Debye length out from the surface of the solid body. This part of the sheath will therefore be devoid of dust particles as they will either fall down, escape completely from the solid body or collect and make damped oscillations at stable positions in the outer part of the sheath. With increasing plasma bulk speed towards the surface, the inner unstable part of the sheath will decrease in thickness.

The sources for the dust in the sheath are assumed to be mainly ejecta from meteorites and micrometeorites, but may also, for the smallest solid bodies, be from electrostatic levitation of very small dust particles. We have for different sizes of solid bodies calculated the sizes of ejecta that can be 'floated' in the sheath. For the solar wind plasma, the suspended dust particles range from less than 1 μm for the Moon to about 80 μm for an asteroid with radius 1 km. These particles create a 'dust atmosphere'.

The results in this paper hold when the dust particle density is so low that the charges on the dust particles do not contribute significantly to the total space charge; a higher density will lead to a modification of the sheath.

Our calculations show that ejecta below a certain size will be accelerated in the sheath and totally escape from the body even if they have near zero initial vertical velocity, while ejecta above this size will need a much larger velocity to escape. This is especially significant for the small solid bodies (radius of order km and less) which will therefore act as important sources of micronsized dust. This could be of significance for the dust production and the size distribution of dust in planetary ring systems.

1. Introduction

Dust particles are present in very many astrophysical, planetary and earth phenomena. Dust may be absent or play a minor role especially in dilute and hot media, but in other cases, e.g. comets and planetary rings, dust can be the dominant particle. We also know that dust is abundant on some planetary and moon surfaces, and this may be the case for asteroid surfaces as well. The dust on such surfaces is probably mainly produced by the impact of large and small particles. The physics of impact processes and the effectivity and manner in which dust is produced is not very well known. We also know little about the way the dust behaves after it is produced on these surfaces. The absence of a thick atmosphere on moons and

Earth, Moon, and Planets **56**: 7–34, 1992.

asteroids excludes winds as a means to redistribute dust over the surface as happens on the Earth's and the Martian surface. However, Gold (1955) suggested the possibility of electrostatic charging of the lunar surface and electrostatic dust transport though levitation of dust.

Singer and Walker (1962b) found that the electric field on the sunlit lunar surface is insufficient to levitate dust, but showed that ejected dust after micrometeorite impacts could be 'floated' in the electric field in the plasma sheath above the surface. This would then lead to a substantial amount of lunar dust being transported along the lunar surfaces over cosmological timescales.

There have been many observations of dust near the lunar surface. Several Surveyor spacecraft observed light scattering ('horizon glow') from dust probably only 10–30 cm above the surface of the Moon after the local sunset (Norton *et al.*, 1967; Rennilson 1968; Gault *et al.*, 1968; 1970; Criswell, 1972; Rennilson and Criswell, 1974). Apollo 17 astronauts observed 'streamers' accompanying the local sunset, believed to be light scattering from dust up to 120 km, the altitude of the spacecraft (McCoy and Criswell, 1974). A dust sensor placed on the Moon by the Apollo 17 astronauts detected moving dust above the surface (Berg *et al.*, 1976). The Lunokhod 2 vehicle measured scattered light up to at least 260 m above the lunar surface (Severny *et al.*, 1974).

It appears that impact of micrometeorites does not inject dust fast enough to explain the observation of elevated dust at the local sunset on the Moon (Rennilson and Criswell, 1974). Criswell (1972, 1973), Criswell and De (1977) and De and Criswell (1977) have developed a model where considerable electric fields are created between illuminated and dark parts of the Moon near the terminator, causing levitation of dust.

Mendis *et al.* (1981) discussed the electrostatic charging of the cometary nucleus and showed that submicron particles can be electrostatically levitated and also be totally blown off the cometary surface.

The 'spokes' of Saturn's rings are probably caused by electrostatic levitation of dust from large boulders (Goertz and Morfill, 1983, Morfill and Goertz, 1983).

A solid body in a plasma will be surrounded by a plasma sheath. The type of sheath will depend on factors such as the ambient plasma, the type of the solid body, and on whether the body is illuminated by sufficiently strong ultraviolet light (e.g., Singer and Walker, 1962a; Guernsey and Fu, 1970; Grard and Tunaley, 1971; Fu, 1971; Walbridge 1973; Lafon, 1976; Besse and Rubin, 1980; see also references in Whipple, 1981).

In this paper we will study the dynamics of dust in the plasma sheath above a surface in space, e.g. above the surface of satellites and asteroids and examine the possibilities and conditions of dust suspension in the sheath.

A charged dust particle in a plasma sheath will be acted upon by the electric field in the sheath and the gravitational force from the Moon or the asteroid. The charging of the dust and the surface of the main body is considered to be by impact of electrons and protons. In other words, we study the dust on the dark side

of the moons and asteroids or above all surfaces of objects which are sufficiently far from the Sun or in dense or hot enough plasma environments that the photoelectric effect can be neglected. The results may also be applied to a laboratory plasma with only electric and gravitational forces.

The electric field and the equilibrium charge of a dust particle as functions of the position in the sheath are computed in Sections 2 and 3 and the position where the electric force on a dust particle at charge equilibrium balances the gravitational force is found in Section 4. The charge delay of a moving dust particle is taken into account in Section 5 by numerical solution of the equation of motion and in Section 6 by solving the linearized equation of motion. In Section 7 we compute under which circumstances dust particles ejected from the surface will be 'floated' and come to rest in the sheath and we also discuss possible dust sources for the sheath.

2. The Sheath Model

The conductivity of the lunar surface is very small (Olhoeft *et al.*, 1972) and we assume this to be the case for all the surfaces we consider. We also take the radius of curvature of the surface to be much larger than the Debye length, i.e. we consider one-dimensional thin and collisionless sheaths. The ambient plasma particles are taken to be electrons and protons and we neglect any photoelectric effect.

Since electrons have a much higher thermal velocity than ions, the surface will have a negative potential if we consider an equilibrium situation. The electric potential V in the sheath is determined by Poisson's equation

$$\frac{\mathrm{d}^2V}{\mathrm{d}x^2} = -\frac{e}{\epsilon_0}(n_i - n_e)\,, \tag{1}$$

with the appropriate boundary conditions. Here x is the distance above the surface, e the magnitude of the electronic charge, n_i the ion density, n_e the electron density and ϵ_0 the vacuum permittivity.

We regard the dust particles as test particles and do not include their charge in the total charge density in Equation (1).

We now make an estimate of the Debye sheath potential $V(x)$ (e.g., Chen, 1984) by assuming that the electrons within the sheath have a Boltzmann distribution with density

$$n_e = n_0 \exp\left(\frac{eV}{kT_e}\right); \tag{2}$$

while the ions are cold with a drift velocity $v_{i,\mathrm{dr}}$ into the sheath at its outer part. In Equation (2) n_0 is the ion and electron density far from the surface, T_e the electron temperature and k the Boltzmann constant.

Due to the acceleration in the sheath's electric field the ion density n_i is a function of V of the form

$$n_i = n_0\left(1 - \frac{2eV}{m_i v_{i,\mathrm{dr}}^2}\right), \tag{3}$$

where m_i is the proton mass. We now insert Equations (2) and (3) in Equation (1) and change variables to $Y = eV/kT_e$ and $z = x/\lambda_D$ where λ_D is the Debye length. We further define $\mathcal{M} = v_{i,\mathrm{dr}}/(kT_e/m_i)^{1/2}$, multiply Equation (1) with $Y' = \mathrm{d}Y/\mathrm{d}z$ and integrate to get

$$\frac{1}{2}\left(\frac{\mathrm{d}Y}{\mathrm{d}z}\right)^2 = \mathcal{M}^2\left[\left(1 - \frac{2Y}{\mathcal{M}^2}\right)^{1/2} - 1\right] + \exp(Y) - 1\,, \tag{4}$$

where the boundary conditions $Y(\infty) = 0$ and $Y'(\infty) = 0$ are used.

The drift velocity $v_{i,\mathrm{dr}}$ can be found by a series expansion of Equation (4) for $Y \ll 1$, i.e., in the outer part of the sheath, giving

$$\left(\frac{\mathrm{d}Y}{\mathrm{d}z}\right)^2 = Y^2\left(1 - \frac{1}{\mathcal{M}^2}\right); \tag{5}$$

which for real solutions require $\mathcal{M}^2 \geqslant 1$ or

$$v_{i,\mathrm{dr}} \geqslant \left(\frac{kT_e}{m_i}\right)^{1/2}. \tag{6}$$

This is the so-called Bohm sheath criterion which states that the ions must enter the sheath with at least the ion acoustic velocity $(kT_e/m_i)^{1/2}$.

We may integrate (4) if we know $\mathcal{M}$ and the wall potential V_s. The Maxwellian electron distribution far from the surface is given by

$$f_e(v) = n_0\left(\frac{m_e}{2\pi kT_e}\right)^{3/2} \exp\left(-\frac{m_e v^2}{2kT_e}\right), \tag{7}$$

where m_e is the electron mass. The electron current to the surface, j_e, is due to those electrons which have a velocity towards the surface larger than $v_{e,\min} = (-2eV_s/m_e)^{1/2}$. This gives

$$j_e = -e\int_{v_{e,\min}}^{\infty}\int_{-\infty}^{\infty}\int_{-\infty}^{\infty} v f_e(v)\,\mathrm{d}v_x\,\mathrm{d}v_y\,\mathrm{d}v_x\,. \tag{8}$$

Integration of Equation (8) gives

$$j_e = -n_0 e\left(\frac{kT_e}{2\pi m_e}\right)^{1/2} \exp\left(\frac{eV_s}{kT_e}\right); \tag{9}$$

while the ion current is given by

$$j_i = n_0 e v_{i,\mathrm{dr}} = n_0 e \mathcal{M} \left(\frac{kT_e}{m_i}\right)^{1/2}, \tag{10}$$

Since in equilibrium we must have $j_e + j_i = 0$ we find from Eqs. (9) and (10)

$$\frac{eV_s}{kT_e} = -2.84 + \ln \mathcal{M}. \tag{11}$$

The surface potential is determined by the Mach number $\mathcal{M}$ and the electron temperature.

On surfaces which are directly accessible to the solar wind, we expect that the value $v_{i,\mathrm{dr}}$ is determined mainly by the solar wind velocity, giving on the average $\mathcal{M} \approx 5$ (e.g. Holzer, 1979) and $eV_s/kT_e \approx -1$ for normal incidence of the solar wind. If the solar wind impacts with an angle of incidence ϕ, the ion current to the surface will be determined by $v_{i,\mathrm{dr}} \cos\phi$ and $\mathcal{M}$ in Equation (11) is to be replaced by $\mathcal{M} \cos\phi$. However, the minimum value for $\mathcal{M}$ will be 1 because of the Bohm criterion.

The drift of electrons is neglected because the electron thermal velocity is usually much larger than the solar wind speed. In regions with only thermal ions and electrons, which should be the case for moons within planetary magnetospheres, which are shielded from the solar wind, we expect $\mathcal{M} = 1$ (stationary plasma) unless the difference between the orbital velocity of the moon and the plasma planetary corotating velocity is large. In such cases we can have $\mathcal{M} > 1$.

In regions where the solar wind cannot impact directly, conditions may be quite different and an initial depletion of ions, in the same manner which has been proposed for the dark side of cometary nuclei (Mendis *et al.*, 1981), could lead to substantial negative surface potentials. We do not consider such situations here.

3. Dust Equilibrium Charges in the Sheath

We now consider a spherical dust particle with radius $a \ll \lambda_D$ in the plasma sheath. The electric field of the dust particle will then be practically identical to the Coulomb field. We assume that the dust particles are charged by plasma impacts only and we consider Maxwellian electrons and cold ions as before.

The dust surface potential U is defined to be the relative potential between the local plasma and the surface of the dust particle, that is $U = \Phi - V$ where Φ the absolute dust potential referred to infinity.

The electron current to a dust particle in the sheath is given by a Maxwellian distribution of electrons having gone through a potential V. This current is given by

$$I_e = -n_0 e \pi a^2 \left(\frac{8kT_e}{\pi m_e}\right)^{1/2} \exp\left(\frac{eV}{kT_e}\right) \exp\left(\frac{eU}{kT_e}\right) \quad \text{for } U \leqslant 0, \tag{12a}$$

$$I_e = -n_0 e \pi a^2 \left(\frac{8kT_e}{\pi m_e}\right)^{1/2} \exp\left(\frac{eV}{kT_e}\right)\left(1 + \frac{eU}{kT_e}\right) \quad \text{for } U \geqslant 0\,, \tag{12b}$$

(for their calculation see Havnes *et al.*, 1987).

The ions which approach the sheath with a drift velocity $v_{i,\mathrm{dr}}$ are accelerated in the sheath to a velocity v_i, at potential V according to the equation

$$\tfrac{1}{2} m_i v_i^2 + eV = \tfrac{1}{2} m_i v_{i,\mathrm{dr}}^2\,. \tag{13}$$

As the ion with the local velocity v_i approaches a dust particle of surface potential U its velocity is given by

$$\tfrac{1}{2} m_i v_i^2 = \tfrac{1}{2} m_i v_{i,s}^2 + eU\,; \tag{14}$$

while conservation of angular momentum of the ion with respect to the dust particle leads to

$$v_i b = v_{i,s} a\,, \tag{15}$$

where b is the impact parameter and $v_{i,s}$ is the velocity for an ion which just barely collides with the dust particle. Equations (13), (14) and (15) give for the ion current to the dust particle

$$I_i = n_0 e v_{i,\mathrm{dr}} \sigma_i = n_0 e \pi a^2 \mathcal{M} \left(\frac{kT_e}{m_i}\right)^{1/2} \left(1 - \frac{2eU/kT_e}{\mathcal{M}^2 - 2eV/kT_e}\right), \tag{16}$$

where the ion collision cross-section is $\sigma_i = \pi b^2$.

We have assumed that the effective sticking coefficient for electrons and ions are $S_e = S_i = 1$, i.e. the production of secondary electrons (e.g. Draine and Salpeter, 1979) is neglected.

The total (net) current to the dust particle is given by

$$\frac{\mathrm{d}Q}{\mathrm{d}t} = I_\mathrm{e} + I_i\,. \tag{17}$$

The equilibrium dust charge, which we denote by Q_eq is found by setting

$$I_e + I_i = 0\,. \tag{18}$$

The relation between dust charge Q and dust surface potential U is

$$U = \frac{Q}{4\pi\epsilon_0 a}\,.$$

The relative equilibrium dust potential eU_eq/kT_e as a function of the relative plasma potential eV/kT_e can be found by using Equations (12a), (12b) and (16) in (18). Solving Equation (4) with boundary condition (11) we obtain eV/kT_e as a function of z. By combining these solutions we will also find eU_eq/kT_e as a

function of z. Figure 1 shows the relative plasma potential eV/kT_e and the relative equilibrium dust potential eU_{eq}/kT_e as a function for z for $\mathcal{M} = 1$ and $\mathcal{M} = 5$.

4. Forces on Dust Particles in the Sheath

If a dust particle of given charge Q is placed in the sheath it will be acted upon by electric and gravitational forces and the net force (positive direction outwards) on the dust particle is

$$F_n = m_d \frac{d^2x}{dt^2} = 4\pi\epsilon_0 a U \frac{dV}{dx} - m_d g$$

or

$$F_n = m_d \lambda_D \frac{d^2z}{dt^2} = -4\pi a(\epsilon_0 n_0 e)^{1/2} \left(\frac{kT_e}{e}\right)^{3/2} Y_d \frac{dY}{dz} - m_d g\,, \tag{19}$$

where we have defined $Y_d = eU/kT_e$. The mass of the dust particle is $m_d = \frac{4}{3}\pi \rho_d a^3$, where ρ_d is the material density of the dust particle. As we have assumed a thin sheath model, i.e., the radius R of the solid body is much larger than the Debye length, the gravitational acceleration g is taken to be constant in the sheath.

The size of a dust particle a_{bal} which is in force equilibrium at z, is found by setting $F_n = 0$ in Equation (19). This gives

$$a_{bal} = \left(-\frac{3(\epsilon_0 n_o e)^{1/2}(kT/e)^{3/2} Y_d\, dY/dz}{g\rho_d}\right)^{1/2}. \tag{20}$$

Figure 2 shows the net force at charge equilibrium, $F_{n,eq}$, as a function of z for $\mathcal{M} = 1$ and 5, different dust particle radii and $R = 1$ km. Figure 3 shows the corresponding radius, $a_{bal,eq}$, of the balancing dust particles at charge equilibrium as a function of z for $R = 1$ km and $R = 5$ km. We have in this section assumed a material density of the dust particle of 1000 kg m^{-3}, a mass density (ρ_M) of the solid body of 2300 kg m^{-3} (the assumed density of the largest asteroids), $kT_e = 50$ eV, $kT_i = 0$ and $n_0 = 5 \cdot 10^6$ m^{-3}. For these parameters and $\mathcal{M} = 1$ the maximum dust particle radius, $a_{max,eq}$, will be 81 μm for $R = 1$ km, and 8.1 μm for $R = 100$ km. For the Moon with $g = 1.6$ m s^{-2}, $a_{max,eq} = 1.6$ μm.

At charge equilibrium and $\mathcal{M} = 1$, Figure 2 shows that for dust sizes above the maximum size ($a_{max,eq}$) there will nowhere in the sheath be an electrostatic lifting force large enough to balance the dust particle. For smaller particles there are two balancing points. The inner is unstable because $dF_{n,eq}/dz$ is positive which means that a small perturbation in position from the balancing position will lead to a force pointing away from this position. The outer position is stable. For still smaller dust particles there is no inner unstable point, only one stable outer point.

The position between the stable and unstable part of the sheath is where the force $F_{n,eq}$ has its maximum. From Equation (19) we get

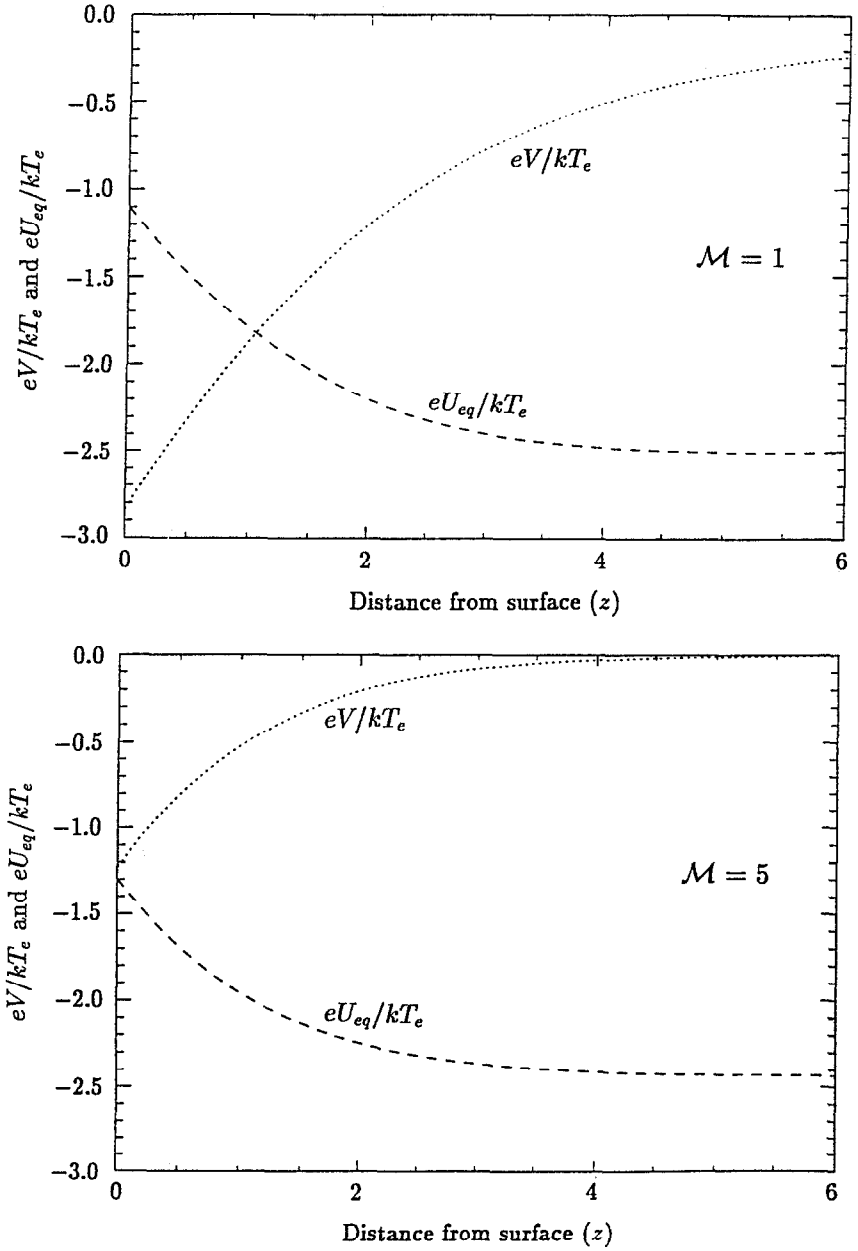

Fig. 1. Relative plasma sheath potential eV/kT_e and relative dust equilibrium potential eU_{eq}/kT_e as functions of distance from the surface for $\mathcal{M} = 1$ and $\mathcal{M} = 5$.

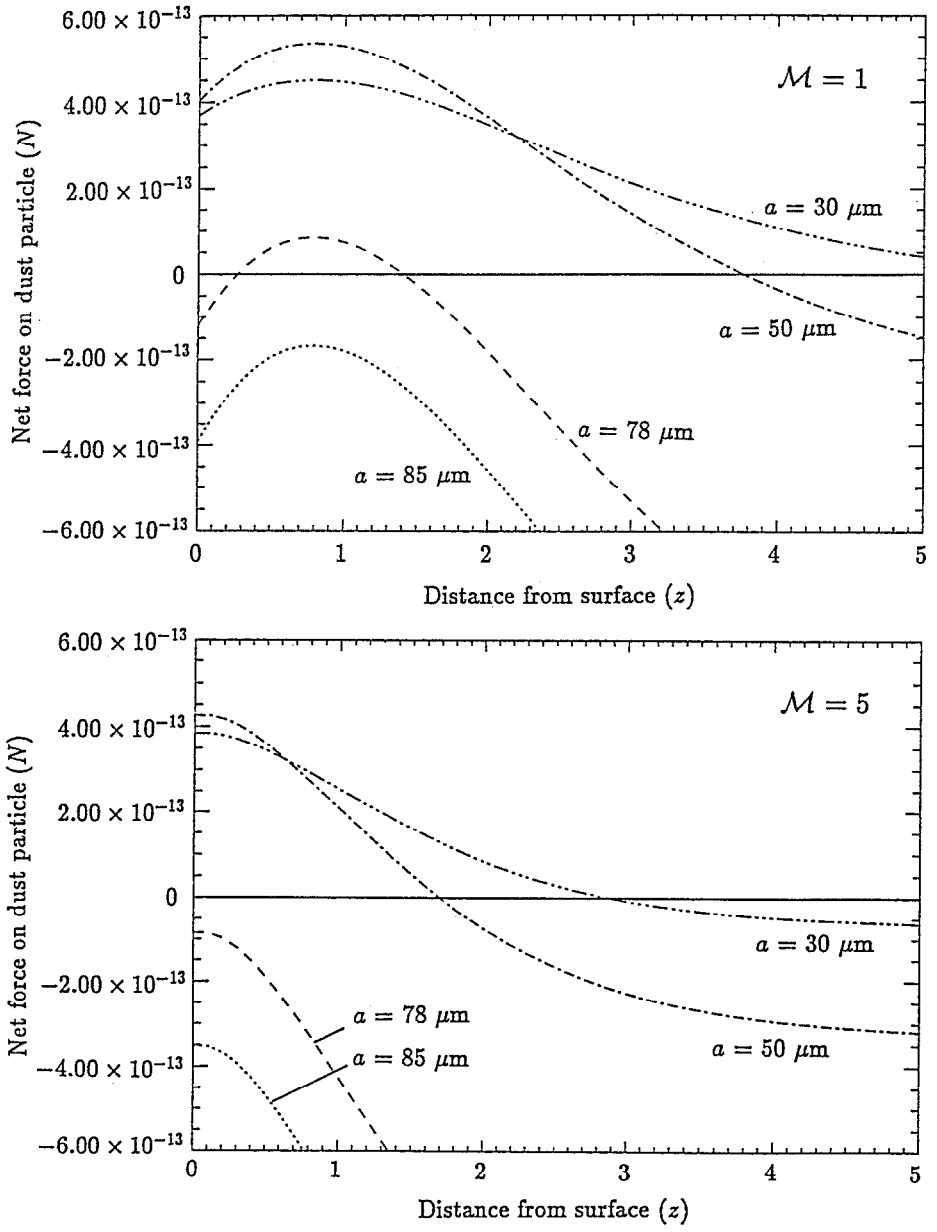

Fig. 2. Net force on a dust particle at charge equilibrium for different dust particle radii in a plasma sheath as a function of distance from the surface. The curves are for $a = 85\ \mu m$, $a = 78\ \mu m$ and $a = 30\ \mu m$ and for $\mathcal{M} = 1$ and $\mathcal{M} = 5$. Other parameters: $R = 1$ km, $\rho_M = 2300\ kg\ m^{-3}$, $\rho_d = 1000\ kg\ m^{-3}$, $n_0 = 5 \cdot 10^6\ m^{-3}$ and $kT_e = 50$ eV.

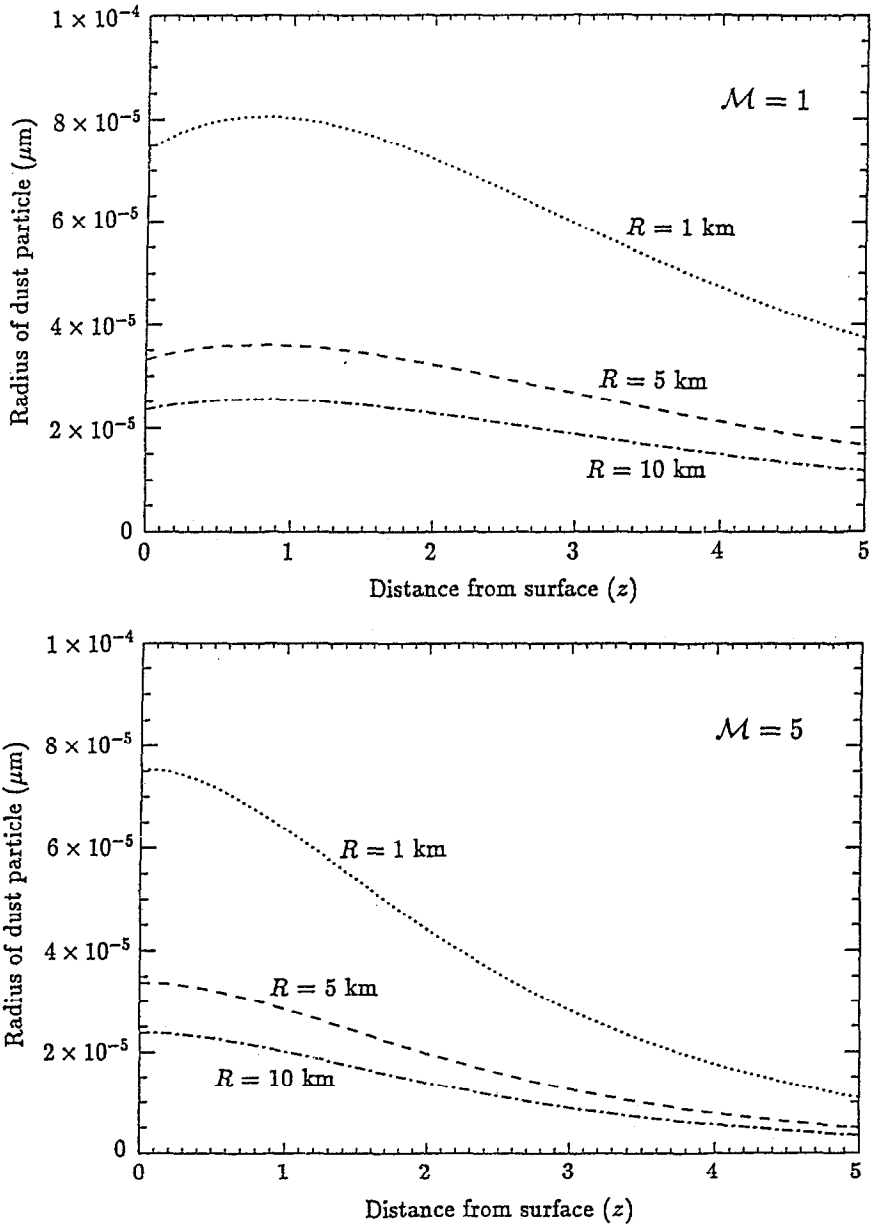

Fig. 3. Radius of balancing dust particle at charge equilibrium in a plasma sheath as a function of distance from the surface. The curves are for solid bodies with $R = 1$ km, $R = 5$ km, $R = 10$ km and for $\mathcal{M} = 1$ and $\mathcal{M} = 5$. Other parameters: $\rho_M = 2300\,\mathrm{kg\,m^{-3}}$, $\rho_d = 1000\,\mathrm{kg\,m^{-3}}$, $n_0 = 5 \cdot 10^6\,\mathrm{m^{-3}}$ and $kT_e = 50$ eV.

$$\frac{dF_{n,eq}}{dz} = -4\pi a(\epsilon_0 n_0 e)^{1/2}\left(\frac{kT_e}{e}\right)^{3/2}\frac{d}{dz}\left(Y_{d,eq}\frac{dY}{dz}\right). \tag{21}$$

We see that $F_{n,eq}(z)$ will have its maximum where $|Y_{d,eq}(dY/dz)|$ has its maximum. From Equation (20) we see that this is also where we find the largest dust particles. The position in the sheath where $F_{n,eq}(z)$ has its maximum we denote by z_c and call this the *critical point*. The critical point will always be at the same z-value regardless of plasma density, electron temperature or g because $|Y_{d,eq}(dY/dz)|$ is independent on these parameters. However, the critical point will be dependent on $\mathcal{M}$. For increasing $\mathcal{M}$, z_c will decrease. Figures 2 and 3 show that $z_c(\mathcal{M} = 1) \approx 0.8$ (stationary plasma) and $z_c(\mathcal{M} = 5) \approx 0$.

We can therefore conclude that if the dust particles are always at charge equilibrium the plasma sheath inside z_c should be devoid of dust particles. Dust particles here will either fall down or be accelerated outward.

If the motion of a dust particle in the sheath is very slow, the dust charge will at any position obtain a value which is close to the local equilibrium charge $Q_{eq}(z)$ but for a fast motion or oscillation the charge will not have sufficient time to adjust and the charge could remain nearly constant.

Linearizing the force Equation (19) around a force balance point z_0 we obtain the oscillation frequency

$$\omega = \left[-\frac{1}{m_d}\left(\frac{dF_n}{dz}\right)_{z_0}\right]^{1/2}. \tag{22}$$

The oscillation period if the dust charge is always at charge equilibrium becomes

$$\tau_{eq} = 2\pi\left[-\frac{g}{\lambda_D}\left(\frac{dY_{d,eq}/dz}{Y_{d,eq}} + \frac{d^2Y/dz^2}{dY/dz}\right)_{z_0}\right]^{-1/2}; \tag{23}$$

while the period for constant charge (equal to the equilibrium charge at z_0) becomes

$$\tau_c = 2\pi\left(-\frac{\lambda_D}{g}\frac{dY/dz}{d^2Y/dz^2}\right)^{1/2}_{z_0}. \tag{24}$$

Figure 4 shows an example of these two limiting oscillation periods as function of position in the sheath for $g = 6.4 \cdot 10^{-4}\,\mathrm{m\,s^{-2}}$ ($R = 1\,\mathrm{km}$), $\lambda_D = 23.5\,\mathrm{m}$ (corresponding to $n_0 = 5 \times 10^6\,\mathrm{m^{-3}}$ and $kT_e = 50\,\mathrm{eV}$) and $\mathcal{M} = 1$. In the case when the charge is always equal to the local equilibrium value, there are no oscillations for $z < z_c \approx 0.8$. τ_{eq} corresponds to zero charge delay and τ_c to an infinite charge delay. However, in a real situation there will always be a finite degree of charge delay.

By solving Equation (17) numerically, we can find the speed with which dust particles are charging and Figure 5 shows calculation for a dust particle of radius

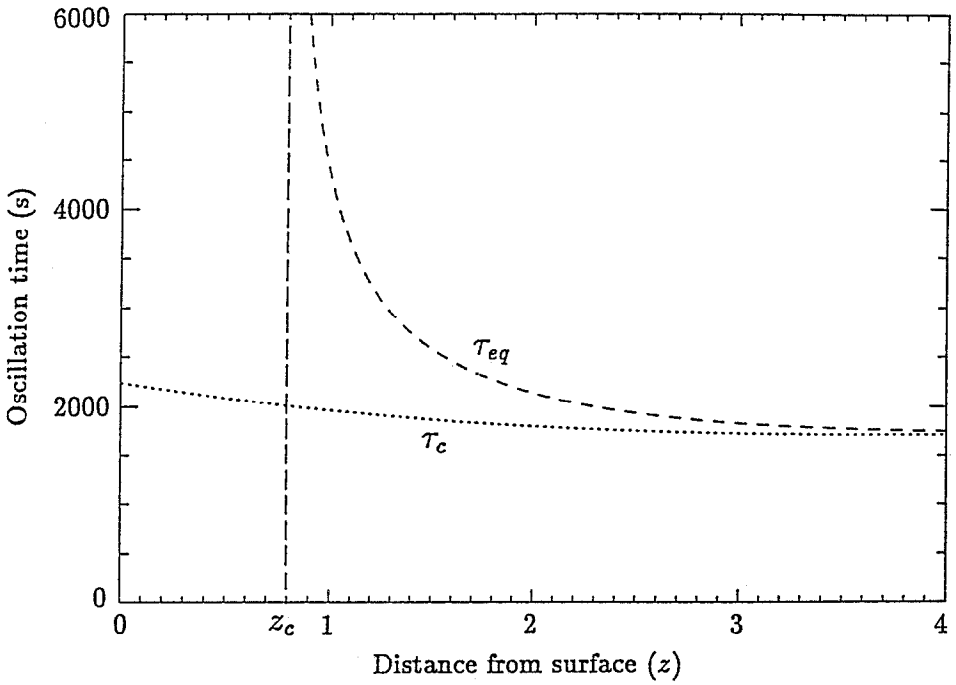

Fig. 4. Period of small oscillation for a dust particle at charge equilibrium (τ_{eq}) and at constant charge (τ_c) as a function of distance from the surface. $R = 1$ km, $\lambda_D = 23.5$ m (corresponding to $n_0 = 5 \cdot 10^6\ \mathrm{m}^{-3}$ and $kT_e = 50$ eV) and $\mathcal{M} = 1$.

1 μm, initially at $U = 0$, for different values of eV/kT_e, i.e., at different positions in the sheath. The time for a dust particle to be charged to half the equilibrium potential is almost independent of the starting potential, and increases with z because the electron density shows the same dependency. From Equation (12a) (neglecting the ion current) we may make a rough estimate of the charging time for $\mathcal{M} = 1$. Assuming $eV/kT_e = 0$,, an average value of eU/kT_e of -1.25, an initial dust potential eU/kT_e of zero and a final dust potential of -2.5, yields

$$t_{\mathrm{ch}} = 4.1 \cdot 10^3 \left(\frac{T_{\mathrm{eV}}}{50_{\mathrm{eV}}}\right)^{1/2} \left(\frac{a_\mu}{1\ \mu\mathrm{m}}\right)^{-1} \left(\frac{n_0}{5 \cdot 10^6\ \mathrm{m}^{-3}}\right)^{-1} \mathrm{s}\,, \tag{25}$$

where T_{eV} is the electron temperature in eV and a_μ is the dust particle radius in μm.

When g increases we see from Equation (20) that the balancing radius decreases and from Equation (25) this leads to an increased charging time. On the other hand, because of Equations (23) and (24), we expect that an increase in g leads to a decrease in oscillation time. This means that when g increases the charge delay for an oscillating dust particle will also increase.

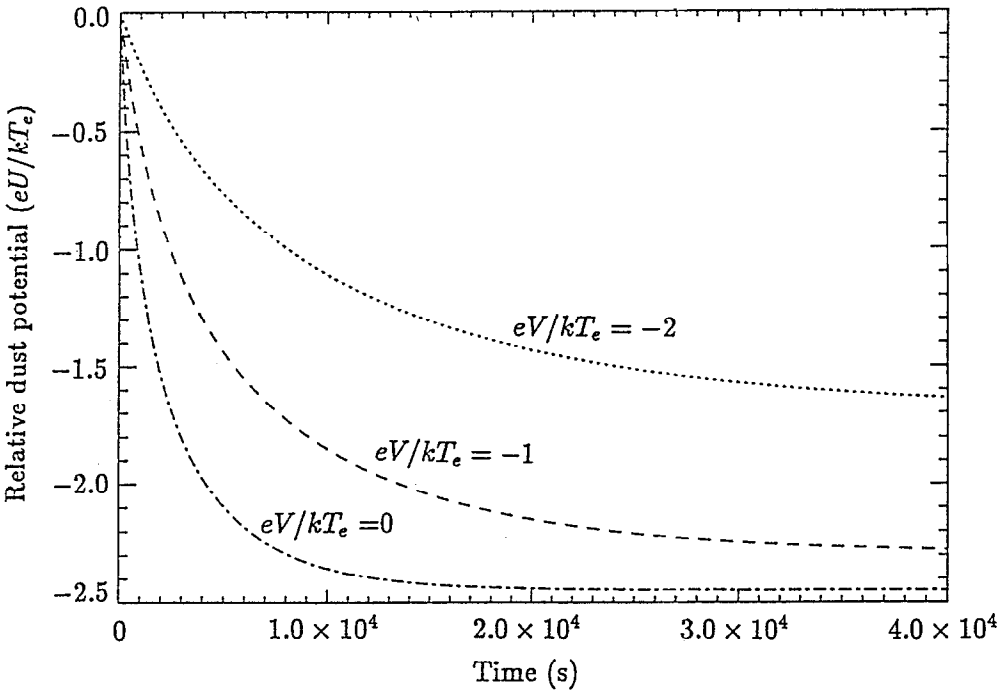

Fig. 5. Relative dust potential eU/kT_e as a function of time for a stationary dust particle with $a = 1\ \mu$m at 3 different positions in the sheath corresponding to the relative plasma potentials $eV/kT_e = 0$, $eV/kT_e = -1$ and $eV/kT_e = -2$. Other parameters: $\mathcal{M} = 1$, $n_0 = 5 \cdot 10^6\ \mathrm{m}^{-3}$ and $kT_e = 50$ eV.

For increasing plasma temperature, Equations (23), (24) and (25) show that both the charging time and the oscillation time increase, and for increasing plasma density both the charging time and the oscillation time decrease. This shows that a change in plasma temperature or density will have a much smaller effect on the charge delay than a change in gravitation.

For a relative large g, when the charge delay is significant and the charge is nearly constant during one oscillation, the force on the dust particle will mainly be a function of the electric field. As the magnitude of the electric field decreases with increasing z, $\mathrm{d}F_n/\mathrm{d}z$ will be negative, making oscillatory motion possible also in the inner part of the sheath. From the results in the next sections it turns out that this will be the case for $g > 6 \cdot 10^{-4}\ \mathrm{m\,s^{-2}}$. For $g < 6 \cdot 10^{-4}\ \mathrm{m\,s^{-2}}$ an increasing part of the sheath inside z_c will not allow oscillations because $\mathrm{d}F_n/\mathrm{d}z$ will be positive, and for $g < 2 \cdot 10^{-4}\ \mathrm{m\,s^{-2}}$ this will apply for all $z < z_c$.

When dust particles oscillate in the inner part of the sheath (inside z_c) it could be suspected that this region might possibly *not* be devoid of dust particles as in the case of charge equilibrium (when there can be no oscillations in the inner part of the sheath). In the next sections we will show that the inner part of the sheath will be devoid of particles in all cases, regardless of the degree of the charge delay.

We will show this both by numerical solutions of the full set of equations and by solving the linearized set of equations.

5. Dynamics of Dust in the Sheath. Solution of the Equation of Motion

We will now examine the motion of dust particles of given sizes which are injected into the sheath from the surface with different initial vertical velocities and charges. The motion is determined by the equation of motion (19) and the current Equation (17) in which we use Equations (12a), (12b) and (16). These equations may be written as

$$\ddot{z} = \frac{\mathrm{d}^2 z}{\mathrm{d}t^2} = \ddot{z}(z, Y_d)\,, \tag{26}$$

$$\dot{Y}_d = \frac{\mathrm{d}Y_d}{\mathrm{d}t} = \dot{Y}_d(z, Y_d)\,.$$

The solution of this system of nonlinear differential equations is first solved numerically to give us $z(t) = x(t)/\lambda_D$ and $Y_d(t) = eU(t)/kT_e$, which represent the relative position and relative potential of the dust particle, as function of time when the initial conditions are given.

The fate of an injected dust particle will be one of three possibilities:

1. It falls back to the surface,
2. it may totally escape, or
3. it may be suspended ('floated') in the sheath.

The last possibility may come about in two different ways, either the dust particle is captured by the sheath directly, or it may first escape from the sheath, be charged in the plasma outside the sheath and then be sufficiently decelerated by the electric field on the way back to be captured by the sheath.

Figure 6 shows an example of an orbit above the surface of a solid body with $R = 1$ km and $\mathcal{M} = 1$.

We observe the following from our numerical computations (of which Figure 6 is an example):

1. The period of oscillation increases with decreasing g as expected from the discussion in Section 4. The period of oscillation will be between τ_{eq} and τ_c as found in the previous section.
2. There is a charge delay which can be seen as a phase shift between the oscillations of the actual dust potential (eU/kT_e) and the equilibrium dust potential (eU_{eq}/kT_e). There is a corresponding phase shift between the position (z) and the actual dust potential.
3. The oscillations are always damped and the dust particle will eventually settle down at its outer balancing position.

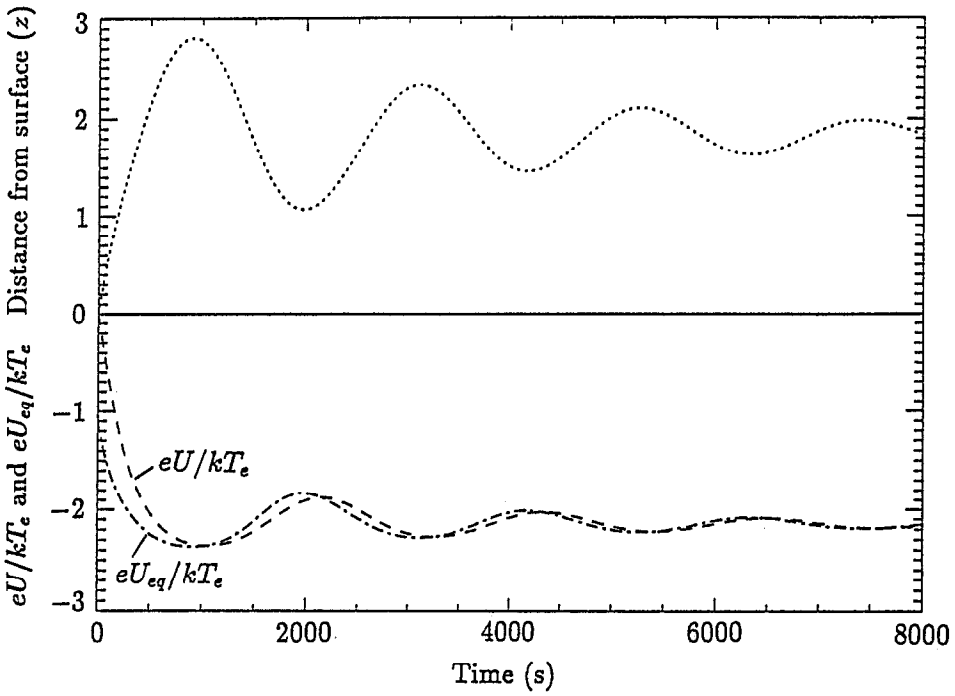

Fig. 6. Oscillation of a dust particle of radius 74 μm in a plasma sheath above the surface of a solid body with $R = 1$ km. The upper part of the figure shows the distance from the surface as a function of time and the lower part shows the relative dust particle potential and the relative equilibrium dust particle potential. The dust particle was injected from the surface with a velocity of 15% of the escape velocity and with zero charge. Other parameters: $\mathcal{M} = 1$, $\rho_M = 2300\,\mathrm{kg\,m^{-3}}$, $\rho_d = 1000\,\mathrm{kg\,m^{-3}}$, $n_0 = 5 \cdot 10^6\,\mathrm{m^{-3}}$ and $kT_e = 50$ eV.

An inner balancing point (inside z_c) is unstable and in all our numerical examples a perturbed dust motion results in that either the dust particle falls back to the surface, or moves out to the outer balancing point.

Two questions arise: Will there always be damping of the oscillations, and will the oscillations in the inner part of the sheath always be unstable? To answer these questions, at least for small oscillations, we will linearize Equations (26).

6. Linearized Solution of the Equation of Motion

To linearize Equations (26) we expand the functions $\ddot{z} = \ddot{z}(z, Y_d)$ and $\dot{Y}_d = Y_d(z, Y_d)$ as first order Taylor polynoms about chosen points z_0 and Y_{d_0}. If we set $z = z_0 + z_1$ and $Y_d = Y_{d_0} + Y_{d_1}$ where z_1 and Y_{d_1}, are small perturbations, the linearized equations are

$$\ddot{z}(z, Y_d) = \ddot{z}(z_0, Y_{d_0}) + \frac{\partial \ddot{z}}{\partial z}(z_0, Y_{d_0}) z_1 + \frac{\partial \ddot{z}}{\partial Y_d}(z_0, Y_{d_0}) Y_{d_1}\,, \tag{27}$$

$$\dot{Y}_d(z, Y_d) = \dot{Y}_d(z_0, Y_{d0}) + \frac{\partial \dot{Y}_d}{\partial z}(z_0, Y_{d0}) z_1 + \frac{\partial \dot{Y}_d}{\partial Y_d}(z_0, Y_{d0}) Y_{d_1} .$$

If we define

$$\frac{\partial \ddot{z}}{\partial z}(z_0, Y_{d0}) \equiv a_2 , \tag{28}$$

$$\frac{\partial \ddot{z}}{\partial Y_d}(z_0, Y_{d0}) \equiv c_2 , \tag{29}$$

$$\frac{\partial \dot{Y}_d}{\partial z}(z_0, Y_{d0}) \equiv a_3 , \tag{30}$$

$$\frac{\partial \dot{Y}_d}{\partial Y_d}(z_0, Y_{d0}) \equiv c_3 \tag{31}$$

and

$$\dot{z} \equiv u_1 ,$$

Equations (27) can be written as the linear system

$$\begin{aligned} \dot{z}_1 &= u_1, & z_1(0) &= z_{10} , \\ \dot{u}_1 &= a_2 z_1 + c_2 Y_{d_1}, & u_1(0) &= u_{10} , \\ \dot{Y}_{d_1} &= a_3 z_1 + c_3 Y_{d_1} , & Y_{d_1}(0) &= Y_{d10} ; \end{aligned} \tag{32}$$

where z_{10}, u_{10} and $Y_{d_{10}}$ are the initial values.

The characteristic equation for this system is

$$\lambda^3 - c_3\lambda^2 - a_2\lambda + a_2 c_3 - a_3 c_2 = 0 . \tag{33}$$

According to the theory of linear differential equations, oscillatory motion requires complex roots of the characteristic Equation (33). In this case the solutions $z_1(t)$, $u_1(t)$ and $Y_{d_1}(t)$ can be written as different linear combinations of

$$e^{\lambda_1 t} \quad \text{and} \quad e^{\mathrm{Re}(\lambda_2)t} \sin(|\mathrm{Im}(\lambda_2)|t + \delta_i) , \tag{34}$$

where $\mathrm{Re}(\lambda_2)$ and $\mathrm{Im}(\lambda_2)$ are the real and imaginary parts of one of the complex conjugate roots and λ_1 is the real root of the characteristic equation.

Consequently, the period of oscillation will be

$$\tau = \frac{2\pi}{|\mathrm{Im}(\lambda_2)|} ; \tag{35}$$

and the oscillation will be damped if $\mathrm{Re}(\lambda_2) < 0$ with time constant for damping

$$\eta = \frac{1}{|\mathrm{Re}(\lambda_2)|} . \tag{36}$$

From the solutions (34) it is also clear that the oscillation is stable if $\lambda_1 \leqslant 0$ and unstable if $\lambda_1 > 0$.

δ_i is a phase constant (different for the 3 solutions and independent of the initial conditions). The phase difference $\delta_{Y_d} - \delta_z$ between the dust potential and position is a measure of the charge delay.

From the roots and coefficients of the characteristic Equation (33) we can extract more information about stability and damping of the oscillations: For complex solutions the roots satisfy

$$\lambda_1 + \lambda_2 + \lambda_3 = c_3 \,, \tag{37a}$$

$$\lambda_1\lambda_2 + \lambda_2\lambda_3 + \lambda_1\lambda_3 = -a_2 \,, \tag{37b}$$

$$\lambda_1|\lambda_2|^2 = -(a_2c_3 - a_3c_2) \,, \tag{37c}$$

where λ_1 is the real root and $|\lambda_2|$ is the norm of the complex conjugative roots.

Use of Equation (19) in Equations (28) and (29) gives

$$a_2 = \frac{gY_0''}{\lambda_d Y_0'} \tag{38}$$

and

$$c_2 = \frac{g}{\lambda_D}\frac{1}{Y_{d_0}} \,, \tag{39}$$

where

$$Y_0'' = \frac{\mathrm{d}^2 Y}{\mathrm{d}z^2}(z_0) \quad \text{and} \quad Y_0' = \frac{\mathrm{d}Y}{\mathrm{d}z}(z_0) \,.$$

Figure 1 shows that $Y_0'' < 0$, $Y_0' > 0$ and $Y_{d_0} < 0$. Consequently, a_2 and c_2 will always be negative.

From Equations (31), (12a), (12b) and (16) it is easy to find that c_3 is also always negative. (This means that the current to the dust particle decreases for increasing dust potential and that the dust potential is a stable one.)

To find the condition for a stable oscillation we have to examine the sign of the real root λ_1. Expressing the linearized Equations (32) in the case of charge equilibrium we obtain

$$\begin{aligned} \ddot{z}_1 &= a_2 z_1 + c_2 Y_{d_{1,\mathrm{eq}}}(z_1) \,, \\ \dot{Y}_{d_1} &= a_3 z_1 + c_3 Y_{d_{1,\mathrm{eq}}}(z_1) = 0 \,, \end{aligned} \tag{40}$$

(the equilibrium potential $Y_{d_{1,\mathrm{eq}}}$ will only be a function of z_1). The derivatives of Equations (40) with respect to z (evaluated at z_0) are

$$\left(\frac{\mathrm{d}\check{z}}{\mathrm{d}z}\right)_{z_0,\mathrm{eq}} = a_2 + c_2\left(\frac{\mathrm{d}Y_{d,\mathrm{eq}}}{\mathrm{d}z}\right)_{z_0} \tag{41}$$

and

$$\left(\frac{\mathrm{d}Y_{d,\mathrm{eq}}}{\mathrm{d}z}\right)_{z_0} = -\frac{a_3}{c_3}. \tag{42}$$

Combining Equations (41) and (42) we obtain

$$\left(\frac{\mathrm{d}\check{z}}{\mathrm{d}z}\right)_{z_0,\mathrm{eq}} = a_2 + c_2\left(-\frac{a_3}{c_2}\right) = \frac{1}{c_3}(a_2c_3 - a_3c_2). \tag{43}$$

Using

$$\frac{\mathrm{d}\check{z}}{\mathrm{d}z} = \frac{1}{m_d\lambda_D}\frac{\mathrm{d}F_n}{\mathrm{d}z}$$

(which is found by derivating Equation (19)) and Equation (37c) in Equation (43) we find that

$$\left(\frac{\mathrm{d}F_{n,\mathrm{eq}}}{\mathrm{d}z}\right)_{z_0} = -\frac{\lambda_1|\lambda_2|^2}{m_d\lambda_D c_3}. \tag{44}$$

As c_3 is always negative, Equation (44) show that the derivative of the net force at charge equilibrium has the same sign as the real root of the characteristic equation. We have shown that for oscillatory motion the sign of the real root decides the stability. Inside the critical point in the sheath $\mathrm{d}F_{n,\mathrm{eq}}/\mathrm{d}z$ is positive, and it then follows from Equation (44) that λ_1 is also positive, which means that the oscillation is unstable. Outside the critical point the derivative of the net force is negative which then implies a stable oscillation. These results are valid regardless of the magnitude of the charge delay.

For small oscillations it is easy to show that the oscillations are always damped. If we take the real part of Equations (37) and call the real part of the two complex conjugate roots R we get

$$\begin{aligned} &\lambda_1 + 2R = c_3, \\ &2\lambda_1 R + |\lambda_2|^2 = -a_1, \\ &\lambda_1|\lambda_2|^2 = -(a_2c_3 - a_3c_2). \end{aligned} \tag{45}$$

Elimination of λ_1 and $|\lambda_2|^2$ gives

$$8R^3 - 8c_3R^2 + (2c_3^2 - 2a_2)R + a_3c_2 = 0. \tag{46}$$

In this cubic equation in R we know that c_3 and a_2 are negative. Combining Equations (39) and (42) we find that

$$a_3 c_2 = -\left(\frac{\mathrm{d}Y_{d,\mathrm{eq}}}{\mathrm{d}z}\right)_{z_0} c_3 \frac{g}{\lambda_D} \frac{1}{Y_{d_0}}. \tag{47}$$

In Equation (47) c_3 and Y_{d_0} are always negative. The derivative of the dust potential at charge equilibrium is also negative (see Figure 1). So $a_3 c_2$ will always be positive. This means that Equation (46) has only positive coefficients, so any real solution must be negative. Because the oscillations are damped if the real part of the complex conjugate roots is negative, this shows that the (small) oscillations in the sheath are always damped.

If the dust particle is always at charge equilibrium or at constant charge the force on the particle will only be a function of position, so it will be in a conservative force field. This means that there will be no drain of oscillatory energy. When the dust particle is not in charge equilibrium we have shown that this gives damped oscillations and therefore a loss in energy. The damping of the oscillations will be maximum for a charge delay somewhere between charge equilibrium and constant charge.

7. "Floating" of Injected Dust in the Sheath

We will in this section assume that dust is injected from the surface with some initial charge and vertical velocity. We compute the subsequent motion of the dust particles and determine the initial conditions which lead to dust being stably suspended in the plasma sheath. A short discussion of possible injection mechanisms is given in Section 8.

In order to be stably suspended, a dust particle must not have a radius (or mass, given the density) larger than the maximum we found in Section 4, see also Figure 3. If the dust particle has zero charge when it is injected from the surface, it needs a minimum time in the sheath to be sufficiently charged to prevent it from falling back onto the surface. If the available time is short, e.g., due to a large g, or the charging time is long (e.g., due to low plasma density, low electron temperature or small radius) the probability for suspension will be small.

On the other hand, the initial vertical velocity must not be too great or the dust particle may escape, either because the initial velocity is larger than the escape velocity, or because the acceleration in the sheath adds a sufficient energy to make it escape.

If the time in the sheath is too small for the dust particle to be sufficiently charged, it may in some cases still be suspended if the initial velocity is so large that it will go out of the sheath (but not escape) and then be sufficiently charged outside to be stopped on the way back.

In the following we assume, as before, a dust particle material density $\rho_d = 1000\,\mathrm{kg\,m^{-3}}$, a solid body material density $\rho_M = 2300\,\mathrm{kg\,m^{-3}}$ (except for the Moon), and an electron temperature of $kT_e = 50\,\mathrm{eV}$. We will examine the effect of changing $\mathcal{M}$, g and n_0. We have in the computation assumed the outer limit of

the sheath at $z = 10$, and let the plasma outside this be Maxwellian with an electron and ion temperature of 50 eV. For the case with the smallest gravitation, $g = 6.4 \cdot 10^{-4}\,\mathrm{m\,s^{-2}}$, corresponding to a body of radius $R = 1$ km, we have taken into account the decreasing g in the sheath in order to get a continuous transition to the region outside $z = 10$.

The results for $\mathcal{M} = 1$, $R = 1$ km, $n_0 = 5 \cdot 10^6\,\mathrm{m^{-3}}$ and 3 different initial dust potentials (relative potentials Y_{d_0} −0.5, 0 and +0.5) are shown in Figure 7a–c as 'windows' for the dust radius and initial vertical velocity that leads to suspension in the sheath. Outside this 'window' the parameter regions which lead to escape or falling back are marked. Larger dust particles in the lower right part of the windows are 'directly' suspended, and those to the upper left are suspended after first having left the sheath and then returned.

The initial velocity is given as a fraction of the escape velocity. For $R = 1$ km and 100 km the escape velocity is $1.13\,\mathrm{m\,s^{-1}}$ and $113\,\mathrm{m\,s^{-1}}$ respectively, and for the Moon it is $2.38\,\mathrm{km\,s^{-1}}$.

In Figure 8 we have calculated the 'window' for the same conditions as in Figure 7a, except for $\mathcal{M} = 5$, corresponding to a solar wind flow perpendicular to the surface.

In Figure 9 the calculations are for the same condition as Figure 7a, except that $g = 6.4 \cdot 10^{-2}\,\mathrm{m\,s^{-2}}$ (corresponding to $R = 100$ km). In Figure 10 we have used a denser plasma ($n_0 = 10^8\,\mathrm{m^{-3}}$) and $g = 1.6\,\mathrm{m\,s^{-2}}$ (corresponding to the Moon).

From these 'windows' we see that there are no dust particles above a maximum size $a_{\max}$ that can come to rest within the sheath. For small g this is close to the $a_{\max,\mathrm{eq}}$ we found in Section 4, but for larger g, $a_{\max}$ will be smaller than $a_{\max,\mathrm{eq}}$.

For dust particles with zero or negative initial potentials, we see that for small g (Figures 7 and 8) there will be no dust particles below a minimum size, $a_{\min}$ that can come to rest in the sheath. The reason is that the smaller dust particles will be accelerated in the sheath to velocities above the escape velocity. For larger g (Figures 9 and 10), $a_{\min}$ decreases and could become low enough for field emission to be important. At the temperature of $kT_e = 50$ eV, field emission could have an effect for $a \lesssim 0.1\ \mu$m (e.g. Draine and Salpeter, 1979). Field emission may lead to a rapid breakup of these small dust particles.

If we assume a negative initial dust potential, Figure 7b shows that some of the dust particles can be suspended even with zero initial velocity because the initial electric force is sufficient to counteract the gravitation and lift it to its equilibrium position. If we assume a positive initial potential, Figure 7c shows that some small dust particles at a very high initial velocity will be suspended. This is because these small particles, because of their positive charges, are decelerated in the sheath and the smaller they are, the larger initial velocity they may be given.

Figure 8 shows that for $\mathcal{M} > 1$ the 'window' is shifted to the left because the electric field in the sheath is smaller (see Figure 1).

For g larger than approximately $0.1\,\mathrm{m\,s^{-2}}$ will all dust particles have to leave the sheath in order to acquire a sufficient negative charge if $n_0 = 5 \times 10^6\,\mathrm{m^{-3}}$. For

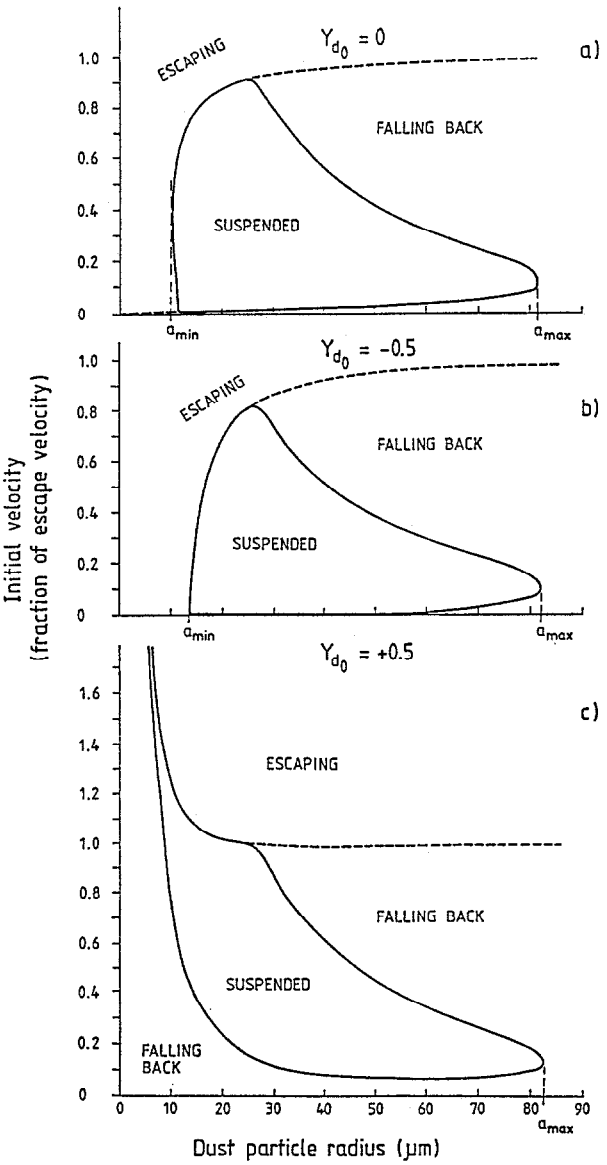

Fig. 7. Windows showing the combinations of initial velocities and dust radii that lead to dust particle suspension in a sheath above the surface of a solid body. $R = 1$ km, $\mathcal{M} = 1$ and the relative initial dust particle potential are 0, −0.5, and +0.5 respectively. The figures also indicate areas for falling back and escape of the dust particles. Other parameters: $\rho_M = 2300\,\mathrm{kg\,m^{-3}}$, $\rho_d = 1000\,\mathrm{kg\,m^{-3}}$, $n_0 = 5 \cdot 10^6\,\mathrm{m^{-3}}$ and $kT_e = 50$ eV.

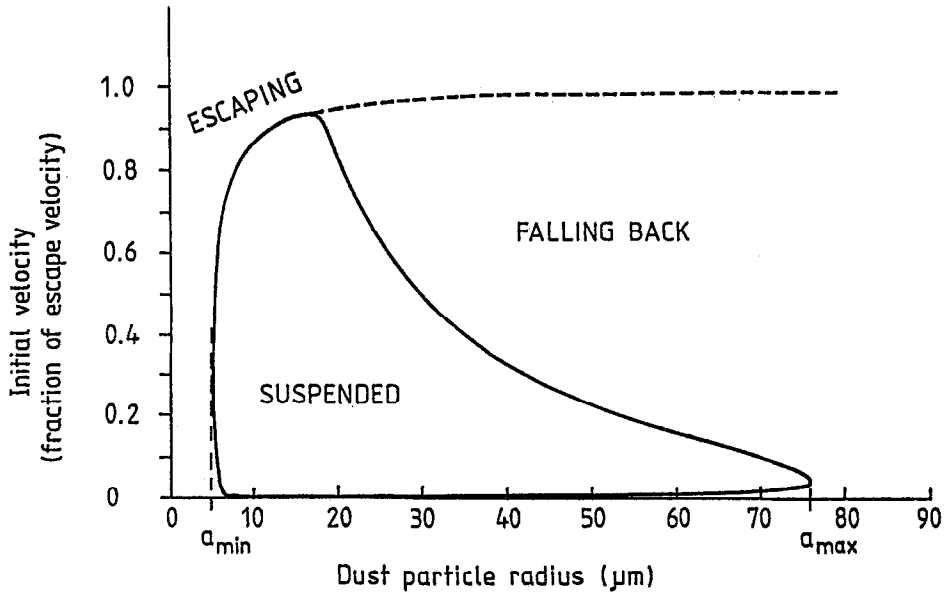

Fig. 8. Window of suspended dust particles for the same conditions as Figure 7a, except that $\mathcal{M} = 5$.

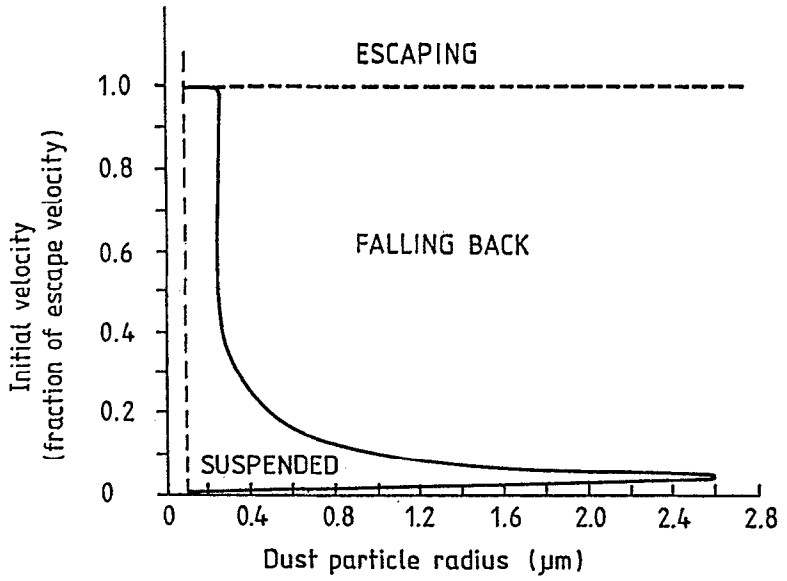

Fig. 9. Window of suspended dust particles for the same conditions as Figure 7a, except that $R =$ 100 km. The vertical dashed line at $a = 0.1$ μm represents the radius where field emission is expected to begin.

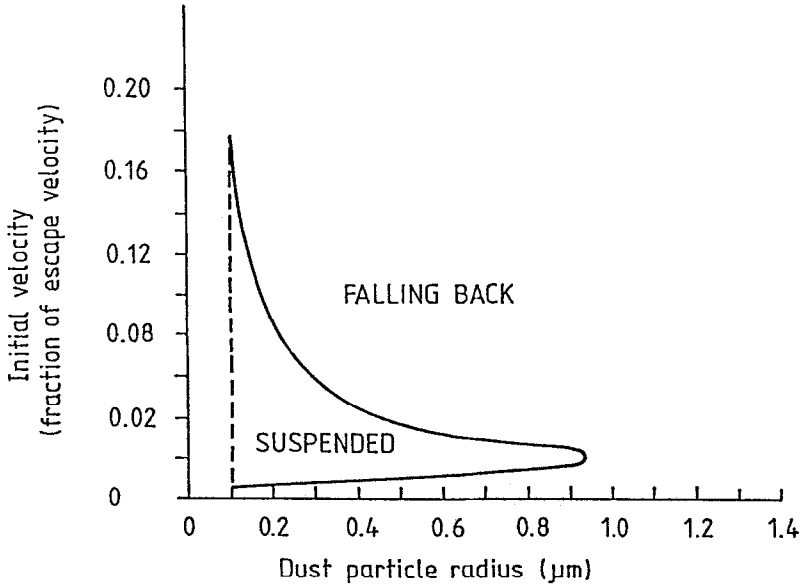

Fig. 10. Window of suspended dust particles for the same conditions as Figure 7a except that $g = 1.6\,\mathrm{m\,s^{-2}}$ (the Moon) and $n_0 = 10^8\,\mathrm{m^{-3}}$. The dashed vertical line at $a = 0.1\,\mu\mathrm{m}$ represents the radius where field emission is expected to begin.

g larger than approximately $1\,\mathrm{m\,s^{-2}}$, a plasma with $n_0 = 5 \times 10\,\mathrm{m^{-3}}$ and electron temperature 50 eV will not charge the dust particles fast enough for suspension if the initial charge is zero. We have therefore used $n_0 = 10^8\,\mathrm{m^{-3}}$ ('high' solar wind density) in Figure 10.

Figure 11 shows $a_{\min}$ as a function of the radius of the solid body for $\mathcal{M} = 1$, $\rho_M = 2300\,\mathrm{kg\,m^{-3}}$, $\rho_d = 1000\,\mathrm{kg\,m^{-3}}$, $n_0 = 5 \cdot 10^6\,\mathrm{m^{-3}}$ and $kT_e = 50\,\mathrm{eV}$. $a_{\min}$ decreases much more rapidly than $a_{\max}$. $a_{\min}$ also increases with increasing plasma density and temperature. The dashed line in the figure is where our sheath model is expected to start to break down because the condition $\lambda_D/R \ll 1$ is no longer satisfied.

The dust particles with radius below $a_{\min}$ will only need a very small initial velocity (of the order of 10^{-2}–$10^{-3}\,\mathrm{m\,s^{-1}}$) to escape; larger dust particles will need an initial velocity close to the escape velocity.

8. Dust Sources

We expect that dust in the sheath above a surface, which could be called a dust 'atmosphere', will be a result of dust particles from the surface. We will consider two mechanisms for this. One is ejecta from meteorite and micrometeorite (primary particle) impacts and the other is electrostatic levitation. Capture of dust from the outside, or condensation of dust within the sheath, due for example to

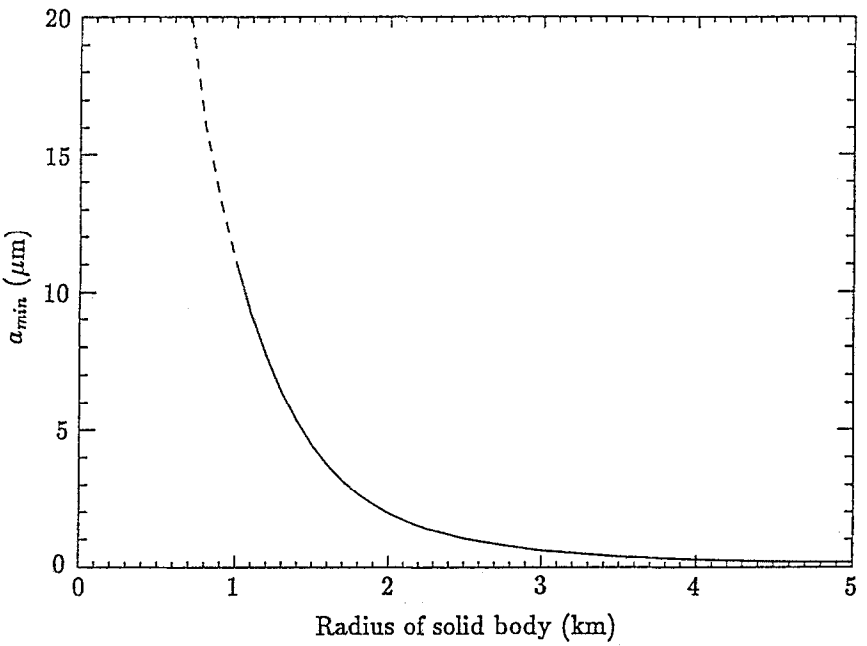

Fig. 11. The minimum dust particle radius, $a_{\min}$ below which all dust particles escape as a function of the radius of the solid body. $\mathcal{M} = 1$, $\rho_M = 2300\ \mathrm{kg\ m^{-3}}$, $\rho_d = 1000\ \mathrm{kg\ m^{-3}}$, $n_0 = 5 \cdot 10^6\ \mathrm{m^{-3}}$ and $kT_e = 50$ eV. The dashed part of the curve is in the region where the thin sheath model starts to break down.

outgassing from the surface, does not appear as a likely source and will not be considered.

Most collisions between primary particles and larger bodies occur with a relative velocity of the order of km/s. Empirical connection between velocity and mass of the primary particle and number, mass and velocity of the ejecta (Dohnanyi, 1969; Gault and Wedekind, 1969; Fujiwara, 1977; see also Grün *et al.* 1984) indicate that most of the ejecta will get a low velocity of the order of m/s, suitable for being suspended in the sheath. Such high velocity collisions, in addition to dust production due to fragmentation, also leads to creation of a plasma cloud and possible charging of the fragments (Grün, 1981). The fragments that are not suspended in the sheath or do not escape, will contribute to the dust on the surface.

By electrostatic levitation of dust we mean that dust particles lying on the surface of a solid body, leave the surface due to electrostatic forces. A dust particle lying on the surface will be a part of that surface and will have a proportional charge as was pointed out by Singer and Walker (1962b). As soon as it leaves the surface the charge will increase towards its 'sheath' value that was found in Section 3. We will briefly examine the condition for levitation.

A spherical dust particle lying on the surface will have the approximate charge

$$Q_s = \sigma \pi a^2 = \frac{E_s}{\epsilon_0} \pi a^2 , \tag{48}$$

where σ is the surface charge density on the body and E_s is the surface electric field strength.

If we use $E_s = 2.47\ \mathrm{V\,m^{-1}}$ taken from our sheath model (Figure 1) for $\mathcal{M} = 1$, we can, by using Equation (48), calculate the number of elementary charges N_s on the dust particle:

$$N_s = 5.3 \cdot 10^{-4} a_\mu^2 , \tag{49}$$

where a_μ is the dust particle radius in μm.

For radii below approximately 43 μm this number will be below unity. As pointed out by others (e.g. Grün *et al.*, 1984) this must be interpreted that only a fraction of micron-sized dust lying on the surface will have one excess charge. To consider levitation for the most relevant dust particle sizes, we must therefore consider dust particles with only one excess charge. The condition for levitation for such a dust particle will be

$$eE_s > \tfrac{4}{3} \pi a^3 \rho_d g \tag{50}$$

or

$$a_\mu g^{1/3} < 4.6 \cdot 10^{-2} , \tag{51}$$

where a_μ is in μm and g is in $\mathrm{m\,s^{-2}}$ and where we have assumed $\rho_d = 1000\ \mathrm{kg\,m^{-3}}$. For the surface of the Moon ($g = 1.6\ \mathrm{m\,s^{-2}}$) the radius of the dust particle must be less than 0.04 μm, so this mechanism is not likely to contribute much to dust in the sheath there. For an asteroid with radius 1 km ($g = 6.4 \cdot 10^{-4}\ \mathrm{m\,s^{-2}}$), the radius of the dust particle must be less than 0.5 μm. We see that for our sheath model, levitation can only be important for small bodies like satellites or asteroids.

The electrostatically levitated dust particles, being smaller than $a_{\min}$ (see previous section) will escape completely from the body.

9. Discussion

In this paper we have examined single dust particle dynamics in a plasma Debye sheath near the surface of solid bodies in space. The bodies are taken to be large compared to the Debye length in the plasma and we have especially considered conditions which could resemble those on planetary system bodies such as small and large asteroids, moons and moonlets. The surfaces are taken to be non-conducting and the ambient plasma conditions equivalent to conditions found in the solar wind or in, at least some, planetary magnetospheres. The photoelectric effect has been ignored in the charging of the surface and the dust. Our calculations are relevant for the shadowed terminator region of the Moon and the asteroids and for the sunlit side of bodies sufficiently far from the Sun or in dense or hot

enough plasma so that photoelectric effects can be neglected. Our calculation does not apply to the wake region on the night side and little is known about the sheath structure there.

We have examined the charging process in detail and solved the equation of motion of the dust particles. The charge delay is more pronounced in a Debye sheath than in a photoelectron sheath, because of the difference in the electron density; in a Debye sheath the dust particles are usually far from being at charge equilibrium. We have shown that many of the important dynamical properties, such as damping and instability of oscillations are due to this charge delay.

One of the interesting results of our work is that for a stationary plasma there should be a dust-free region to about one Debye length out from the surface. Even though there may be a position in this region where gravity and electric forces on the dust balances, we show by perturbation analysis and by nonlinear numerical calculation that no stable equilibrium points exist there. Further above the surface dust can be stably suspended with the largest dust particles closest to the surface.

It is interesting to note that the suspension of dust, and a dust-free region close to the surface, is apparently observed in some plasma etching processes of silicone wafers (Selwyn, 1989) where strong electric fields are created near the walls of the plasma chamber.

In the case when the solar wind impinges on the surface, the picture is somewhat modified. The dust free region will be thinner and the maximum dust size slightly smaller.

If the dust particles are orbiting around the body and enters a sunlit region they will discharge and may fall down. If they enter the wake region on the back side relative to the solar wind, they will probably charge to a higher negative potential and may escape (Mendis, 1981; Mendis *et al.*, 1981).

In our model, we find in principle, that all dust particles smaller than $a_{\max,\mathrm{eq}}$ (Section 4) can be kept stably suspended in the sheath. However, in a dynamical situation where the dust is brought into the sheath from the surface, which is the most likely source of the dust, the maximum size for suspension, $a_{\max}$, will be smaller than $a_{\max,\mathrm{eq}}$. For the chosen plasma parameters (Section 7) we find $a_{\max} \approx 0.9\ \mu\mathrm{m}$ for the Moon and several times $10\ \mu\mathrm{m}$ for small asteroids or moonlets.

The smallest dust particles can be accelerated sufficiently by the electric field in the sheath to escape completely even if the initial vertical velocity is very much smaller than the escape velocity. The sheath will therefore both have an upper $a_{\max}$ and a lower $a_{\min}$ cut-off in dust size and acts like a filter which easily allows dust below $a_{\min}$ to escape. If small asteroids or moons are sources of dust they should most likely eject dust particles below this size.

The values of $a_{\min}$ and $a_{\max}$ decrease with increasing gravity and increase with increasing plasma density and temperature.

Also electrostatic levitation from small bodies may be a source of dust. These dust particles will be smaller than $a_{\min}$ and will consequently escape.

The 'dust atmosphere' according to our model, extends from about one to several Debye lengths above the surface and the small bodies will have the largest dust particles. As the Debye length is $\lambda_D = 23.5(T_{eV}/50_{eV})^{1/2} \times (n_0/(5 \times 10^6\,\mathrm{m}^{-3}))^{-1/2}\,\mathrm{m}$, we expect dust atmospheres on moons and asteroids up to some hundreds of meters.

In a fast collision, like micrometeorite impacts, a small fraction of the ejected particles leave the impact spot at high velocities (Eichhorn, 1976). However, the majority of the dust which is produced will be given quite small velocities and this must be even more the case in the slow collisions which can be expected between small moonlets of 0.1–10 km radius in or close to planetary rings (Cuzzi and Burns, 1988). Many dust particles ejected will have vertical velocities and sizes suitable for being suspended in the sheath and we expect that the sheath will collect a significant amount of dust. The results in this paper hold when the dust particle density is not so high that the charges on the dust particles contribute significantly to the total charge. For micron-sized dust and for the plasma dust parameters we have used, this will happen when the dust density becomes of order 10–100 particles/m^3. A larger dust density must lead to a modification of the sheath.

The collection of dust in the sheath above the surface is probably responsible for much of the dust transport on the surface both on the sunlit and the dark side. Plasma sheath effects must also be of importance for the balance between dust production and loss and for the dust size distribution in many planetary ring systems.

References

Berg, O. E., Wolf, H. and Rhee, J.: 1976, in H. Elsässer and H. Fechtig (eds.), *Interplanetary Dust and Zodiacal Light*, Springer, pp. 233–237.

Besse, A. L. and Rubin, A. G.: 1980, *J. Geophys. Res.* **85**, 2324–2328.

Chen, F. F.: 1984, *Introduction to Plasma Physics and Controlled Fusion*, Vol. I, Plenum Press.

Criswell, D. R.: 1972, *Proc. of the Third Lunar Sci. Conf.* **3**, 2671–2680.

Criswell, D. R.: 1973, in R. Grard (ed.), *Photon and Particle Interactions with Surfaces in Space*, D. Reidel Publ. Comp., Dordrecht, Holland, pp. 545–556.

Criswell, D. R. and De, B. R.: 1977, *J. Geophys. Res.* **82**, 1005–1007.

Cuzzi, J. N. and Burns, J. A.: 1988, *Icarus* **74**, 284–324.

De, B. R. and Criswell, D. R.: 1977, *J. Geophys. Res.* **82**, 999–1004.

Dohnanyi, J. S.: 1969, *J. Geophys. Res.* **74**, 2531–2554.

Draine, B. T. and Salpeter, E. E.: 1979, *Astrophys. J.* **231**, 77–94.

Eichhorn, G.: 1976, *Planet. Space Sci.* **24**, 771.

Fu, J. H. M.: 1971, *J. Geophys. Res.* **7**, 2506–2509.

Fujiwara, A.: 1977, *Icarus* **31**, 277–288.

Gault, D. E. and Wedekind, J. A.: 1969, *J. Geophys. Res.* **74**, 6780–6794.

Gault, D. E., Adams, J. B., Collins, R. K., Kuiper, G. P., O'Keefe, J. A., Phinney, R. A. and

Shoemaker, E. M.: 1968, *Post-Sunset Horizon Glow*, Surveyor Project Final Report – Part II: Science Results.
Gault, D. E., Adams, J. B., Collins, R. K., Kuiper, G. P., Masursky, H., O'Keefe, J. A., Phinney, R. A. and Shoemaker, E. M.: 1970, *Icarus* **12**, 230–232.
Goertz, C. K. and Morfill, G.: 1983, *Icarus* **53**, 219–229.
Gold, T.: 1955, *Mon. Not. Roy. Astron. Soc.* **115**, 585–604.
Grard, R. J. L. and Tunaley, J. K. E.: 1971, *J. Geophys. Res.* **7**, 2498–2505.
Grün, E.: 1981, *Comet Halley Probe*; *Plasma Environment*, ESA-SP-155, pp. 81–90.
Grün, E., Morfill, G. E. and Mendis, D. A.: 1984, in R. Greenberg and A. Brahic (eds.), *Planetary Rings*, Univ. of Arizona Press, pp. 275–332.
Guernsey, R. L. and Fu, J. H. M.: 1970, *J. Geophys. Res.* **75**, 3193–3199.
Havnes, O, Goertz, C. K., Morfill, G. E., Grün, E. and Ip, W.: 1987, *J. Geophys. Res.* **2**, 2281–2287.
Holzer, T. E.: 1979, in E. N. Parker, C. F. Kennel and L. J. Lanzerotti (eds.), *Solar System Plasma Phys.*, North-Holland Publishing Company, Vol. I, pp. 101–176.
Lafon, J.-P. J.: 1976, *Radio Science* **11**, no 5, 483–493.
McCoy, J. E. and Criswell, D. R.: 1974, *Proc. of the Fifth Lunar Conf.* **3**, 2991–3005.
Mendis, D. A.: 1981, in F. D. Kahn (ed.), *Investigating the Universe*, D. Reidel Publ. Company, pp. 353–384.
Mendis, D. A., Hill, J. R., Houpis, L. F. and Whipple, Jr., E. C.: 1981, *Astrophys. J.* **24**, 787–797.
Morfill, G. E. and Goertz, C. K.: 1983, *Icarus* **55**, 111–123.
Norton, R. H., Guinn, J. E., Livingston, W. C., Newkirk, G. A. and Zirin, H.: 1967, *J. Geophys. Res.* **72**, 815–817.
Olhoeft, G. R., Frisillo, A. L. and Strangway, D. W.: 1972 in J. W. Chamberlain and C. Watkins (eds.), *The Apollo 15 Lunar Samples*, Lunar Science Inst., Houston, Tex., p. 477.
Rennilson, J. J.: 1968, JPL Tech. Report 32-1265, pp. 119–121.
Rennilson, J. J. and Criswell, D. R.: 1974, *The Moon* **10**, 121–142.
Selwyn, G. S.: 1989, *J. Vac. Sci. Technol. A* **7**, 2758–2765.
Severny, A. B., Terez, E. I. and Zvereva, A. M.: 1974, *Space Res.* **14**, 603–605.
Singer, S. F. and Walker, E. H.: 1962a, *Icarus* **1**, 7–12.
Singer, S. F. and Walker, E. H.: 1962b, *Icarus* **1**, 112–120.
Walbridge, E.: 1973, *J. Geophys. Res.* **78**, 3668–3687.
Whipple, E. C.: 1981, *Rep. Prog. Phys.* **44**, 1197–1250.